# Binding of Spin-Labeled Galactosides to the Lactose Permease of *Escherichia coli*†

Min Zhao,‡ Tamás Kálai,§ Kálmán Hideg,§ Christian Altenbach,|| Wayne L. Hubbell,|| and H. Ronald Kaback*,‡,||

*Molecular Biology Institute, Departments of Physiology and Microbiology & Molecular Genetics, Howard Hughes Medical Institute; Institute of Organic and Medicinal Chemistry, University of Pécs, H-7643 Pécs, P.O. Box 99, Hungary; and Jules Stein Eye Institute and Department of Chemistry & Biochemistry, University of California, Los Angeles, Los Angeles, California 90095-1662*

*Received May 11, 2000; Revised Manuscript Received July 13, 2000*

ABSTRACT: A series of nitroxide spin-labeled α- or β-galactopyranosides and a nitroxide spin-labeled β-glucopyranoside have been synthesized and examined for binding to the lactose permease of *Escherichia coli*. Out of the twelve nitroxide spin-labeled galactopyranosides synthesized, 1-oxyl-2, 5, 5-trimethyl-2-[3-nitro-4-*N*-(hexyl-1-thio-β-D-galactopyranosid-1-yl)]aminophenyl pyrrolidine ($NNG_6^\beta$) exhibits the highest affinity for the permease based on the following observations: (a) the analogue inhibits lactose transport with a $K_I$ about 7 μM; (b) $NNG_6^\beta$ blocks labeling of single-Cys148 permease with 2-(4′-maleimidylanilino) naphthalene-6-sulfonic acid (MIANS) with an apparent affinity of about 12 μM; (c) electron paramagnetic resonance demonstrates binding of the spin-labeled sugar by purified wild-type permease in a manner that is reversed by nonspin-labeled ligand. The equilibrium dissociation constant ($K_D$) is about 23 μM and binding stoichiometry is approximately unity. In contrast, the nitroxide spin-labeled glucopyranoside does not inhibit active lactose transport or labeling of single-Cys148 permease with MIANS. It is concluded that $NNG_6^\beta$ binds specifically to lac permease with an affinity in the low micromolar range. Furthermore, affinity of the permease for the spin-labeled galactopyranosides is directly related to the length, hydrophobicity, and geometry of the linker between the galactoside and the nitroxide spin-label.

The lactose permease (lac permease)[1] of *Escherichia coli* is a polytopic cytoplasmic membrane protein that catalyzes the stoichiometric symport of galactopyranosides and $H^+$ (reviewed in *1*). Encoded by the *lacY* gene of the *lac* operon (*2*), the permease has been solubilized, purified, reconstituted into proteoliposomes, and shown to be solely responsible for galactoside transport (reviewed in *3*) as a monomer (*4*). All available evidence (reviewed in *5*−*7*) indicates that the molecule contains 12 transmembrane domains connected by hydrophilic loops with the N and C termini on the cytoplasmic side of the membrane.

In a functional permease mutant devoid of native Cys residues, each residue has been replaced with Cys (reviewed in *8*). Analysis of the mutant library with a battery of biochemical and biophysical techniques has led to the following developments (*6*−*9*): (i) The great majority of the mutants are expressed normally in the membrane and exhibit significant activity, and only 6 side-chains are clearly irreplaceable for active transport. (ii) Helix packing, tilts, and ligand-induced conformational changes have been determined. (iii) Positions that are accessible to solvent have been revealed. (iv) Positions where the reactivity of the Cys replacement is increased or decreased by ligand binding have been identified. (v) The permease has been shown to be a highly flexible molecule. (vi) A working model for lactose/$H^+$ symport has been formulated.

† This work was supported in part by NIH Grant DK 51131 to H.R.K. and by grants from the Hungarian National Research Foundation OTKA T030013 to K.H. and NIH Grant EY05216 to W.L.H., as well as the Jules Stein Professor endowment.

* Corresponding author mailing address: HHMI/UCLA 6-720 MacDonald Bldg., Box 951662, Los Angeles, CA 90095-1662. Telephone: (310) 206−5053. Fax: (310) 206-8623. E-mail: RonaldK@HHMI.UCLA.EDU.

‡ Howard Hughes Medical Institute.

§ University of Pécs.

|| University of California.

[1] Abbreviations: lac permease, lactose permease; TSP, thermospray; MIANS, 2-(4′-maleimidylanilino)naphthalene-6-sulfonic acid; EPR, electron paramagnetic resonance; DDM, *n*-dodecyl-β-D-maltoside; $KP_i$, potassium phosphate; TDG, β-D-galactopyranosyl 1-thio-β-D-galactopyranoside; IPTG, *i*-propyl 1-thio-β-D-galactopyranoside.

[2] Nitroxide spin-labeled galactopyranosides are designated as follows: $NNG_6^\beta$, 1-oxyl-2,5,5-trimethyl-2-[3-nitro-4-*N*-(hexyl-1-thio-β-D-galactopyranosid-1-yl)]aminophenyl pyrrolidine; $NNG_2^\beta$, 1-oxyl-2,5,5-trimethyl-2-[3-nitro-4-(*N*-methyl)-*N*-(ethyl-1-thio-β-D-galactopyranosid-1-yl)]aminophenyl pyrrolidine; $PNG_1^\beta$, 1-oxyl-2,2,5-trimethyl-2-[4-S−(methyl thio-β-D-galactopyranosid-1-yl)]phenyl pyrrolidine; $PNG_1^\alpha$, 1-oxyl-2,2,5-trimethyl-2-[4-S−(methyl thio-α-D-galactopyranosid-1-yl)]phenyl pyrrolidine; $NNG_0^\alpha$, 1-oxyl-2,2,5-trimethyl-2-[3-nitro-4-(1-thio-α-D-galactopyranosid-1-yl)]phenyl pyrrolidine; $NNG_0^\beta$, 1-oxyl-2,2,5-trimethyl-2-[3-nitro-4-(1-thio-β-D-galactopyranosid-1-yl)]phenyl pyrrolidine; $BNG_0^\alpha$, 1-oxyl-2,2,5,5-tetramethyl-3-[3-nitro-4-(1-thio-α-D-galactopyranosid-1-yl)]benzoyl-2,5-dihydro-1*H*-pyrrole; $NG_3^\beta$, 1-oxyl-2,2,5,5-tetramethyl-3-[3-(1-thio-β-D-galactopyranosid-1-yl)propen-1-yl]-2,5-dihydro-1*H*-pyrrole; $NG_1^\beta$, 1-oxyl-2,2,5,5-tetramethyl-3-(1-thio-β-D-galactopyranosid-1-yl)methyl-2,5-dihydro-1*H*-pyrrole; $NG_1^\alpha$, 1-oxyl-2,2,5,5-tetramethyl-3-(1-thio-α-D-galactopyranosid-1-yl)methyl-2,5-dihydro-1*H*-pyrrole; $fNG_0^\beta$, 1-oxyl-2,2,5,5-tetramethyl-3-formyl-4-(1-thio-β-D-galactopyranosid-1-yl)-2,5-dihydro-1*H*-pyrrole; $fNG_0^\alpha$, 1-oxyl-2,2,5,5-tetramethyl-3-formyl-4-(1-thio-α-D-galactopyranosid-1-yl)-2,5-dihydro-1*H*-pyrrole.

[3] Nitroxide spin-labeled glucopyranoside is designated as follows: $NNGlu_0^\beta$, 1-oxyl-2,2,5-trimethyl-2-[3-nitro-4-(1-thio-β-D-glucopyranosid-1-yl)]phenyl pyrrolidine.

10.1021/bi001075i CCC: $19.00 
Published on Web 08/23/2000

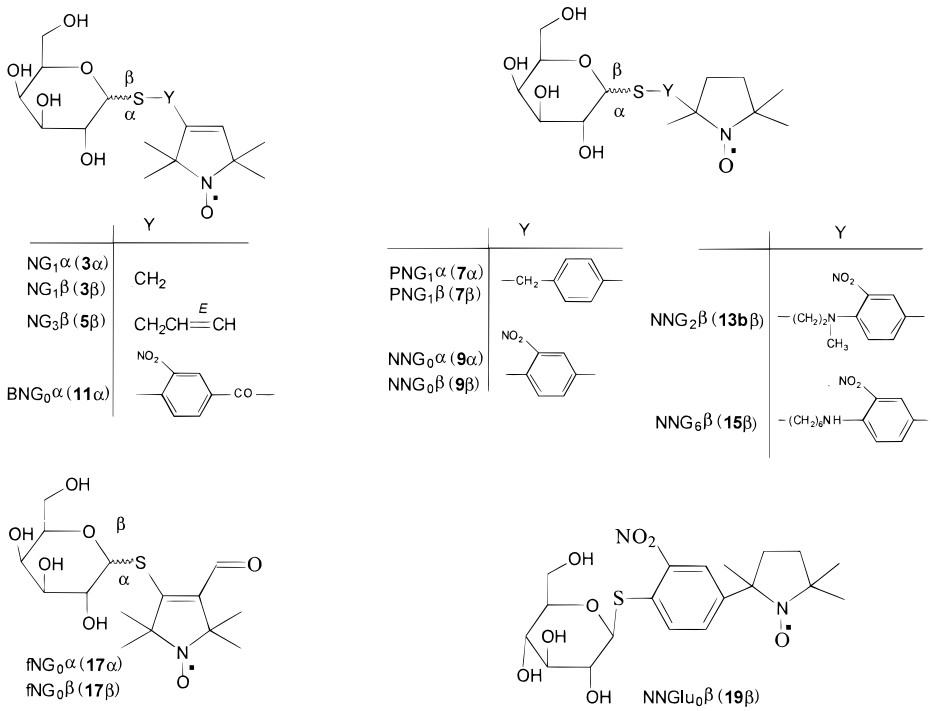


FIGURE 1: Chemical structures of the nitroxide spin-labeled α- or *β*-galactopyranosides and a *β*-glucopyranoside.

On the basis of a detailed characterization of mutants at Cys148 (*10*, *11*), Glu126, and Arg144 (*12*−*15*) and binding studies with a series of galactose analogues (*16*), the following model for galactoside binding was postulated (*8*, *13*): (i) One of the guanidino $NH_2$ groups of Arg144 forms a H-bond with the OH group at the C-4 or C-3 position(s) of the galactosyl moiety of the substrate, an interaction that plays a key role in substrate specificity. (ii) The other guanidino $NH_2$ of Arg144 forms a salt bridge with Glu126, and the interaction holds Arg144 and Cys148 in an orientation that allows specific interaction with the galactosyl moiety. One of the oxygen atoms of the carboxylate at position 126 may also act as an H-bond acceptor from the C-6 OH of the galactosyl moiety, and the C-2 OH is also an important determinant, although both epimers at this position bind to the permease. (iii) Cys148, which is protected by substrate against alkylation by *N*-ethylmaleimide (NEM), interacts hydrophobically with the galactosyl end of lactose and other galactosides. Although interactions with the nongalactosyl moiety are not clearly understood, Met145, which is on the same face of helix V as Cys148, is thought to be important in this respect. In addition, other studies (*17*) indicate that Gly residues in helices IV and V provide the conformational flexibility that is important for substrate binding and transport.

Although major determinants for substrate binding in the permease lie at the interface between helices IV and V, it is virtually impossible to obtain detailed evidence for the binding site model without structure at atomic level. On the other hand, more definitive support for the location of the binding site between helices IV and V might be obtained by means of spectroscopic approaches, and it is this notion that led to the present studies.

We describe here the synthesis and properties of a high-affinity spin-labeled galactopyranoside, 1-oxyl-2,5,5-trimethyl-2-[3-nitro-4-*N*-(hexyl-1-thio-*β*-D-galactopyranosid-1-yl)]aminophenyl pyrrolidine ($NNG_6^{\beta}$), and its properties. Twelve nitroxide spin-labeled α- or *β*-galactopyranosides were synthesized with different linkers between the galactoside and spin-label moiety. Out of the 12, $NNG_6^{\beta}$ binds specifically to the permease with an affinity in the low micromolar range, as demonstrated by transport studies, blockade of 2-(4′-maleimidylanilino)naphthalene-6-sulfonic acid (MIANS) labeling of single-Cys148 permease, and electron paramagnetic resonance (EPR) spectroscopy. In addition, as shown previously (*18*), the affinity of the permease is directly related to the length, hydrophobicity and perhaps the geometry of the linker between the galactoside and spectroscopically active moiety in the analogues.

## EXPERIMENTAL PROCEDURES

*Materials.* Immobilized monomeric avidin was obtained from Pierce (Rockford, IL), [1-$^{14}$C]lactose was purchased from Amersham Pharmacia, Inc. (Uppsala, Sweden), and MIANS was from Molecular Probes, Inc. (Eugene, OR). Compounds **1b**, **14**, and **18** were purchased from Sigma. All other materials were reagent-grade and obtained from commercial sources.

*Synthesis of Spin-Labeled Galactosides (Reviewed in 19).* In general, nitroxide spin-labeled α- or *β*-galactopyranosides and the *β*-glucopyranoside described (Figure 1) were synthesized by aromatic nucleophilic substitution and alkylation reactions between 1-thio-α or *β*-D-galactopyranosides or 1-thio-*β*-D-glucopyranoside sodium salts and nitroxide derivatives. Melting points were determined with a Boetius micromelting point apparatus and are uncorrected. In each case, the IR (Specord 75) spectra were consistent with the assigned structure. Mass spectra were recorded on a VG TRIO-2 instrument with a thermospray (TSP) technique, and samples were analyzed in the bypass mode. The sample solution in $CH_3OH$ (10 *μ*L) was introduced via the thermospray interface. The mobile phase was $CH_3OH/H_2O$ (1:1 by volume) containing 0.1 M $NH_4OAc$. The capillary tip

temperature was 230 °C, the electrode voltage was 180 V, and the source temperature was 210 °C. Flash column chromatography was performed on Merck Kieselgel 60 (0.040−0.063 mm). Qualitative TLC was carried out on commercially prepared plates (20 × 20 × 0.02 cm) coated with Merck Kieselgel $GF_{254}$. Compounds **1α** (20), **2** (*21*), **8**, **10** (*22*), **16** (*23*), tetraacetyl-*β*-D-galactopyranosyl-isothiouronium bromide (*24*), and **13b*β*** ($NNG_2^{\beta}$) (*25*, *26*) were prepared according to published procedures. Synthesis of **4** and **6** will be published elsewhere.

*Alkylation of 1-Thio-D-galactopyranose Sodium Salt. General Procedure (**3α**, **3*β***, **5*β***, **7α**, **7*β***) (Figure 2A).* To a solution of sugar (sodium salt of **1α** or **1*β***; 109 mg, 0.5 mmol) in water (2 mL), a solution of **2**, **4**, or **6** (0.6 mmol) in dioxane (4 mL) was added, and the mixture was refluxed for 30 min. The solvent was evaporated in vacuo, and the residue was purified by flash column chromatography (hexane/EtOAc, $CHCl_3$/MeOH) to give the alkylated product **3α**, **3*β***, **5*β***, **7α**, or **7*β***.

**3α** ($NG_1^{\alpha}$): 50 mg (28%), viscous oil. $R_f$: 0.44 ($CHCl_3$/MeOH, 4:1). IR ($cm^{-1}$) *ν*: 3500−3100, 1620. TSP: 349 $(M+H)^+$

**3*β*** ($NG_1^{\beta}$): 70 mg (40%), viscous oil. $R_f$: 0.42 ($CHCl_3$/MeOH, 4:1). IR ($cm^{-1}$) *ν*: 3500−3100, 1620. TSP: 349 $(M+H)^+$.

**5*β*** ($NG_3^{\beta}$): 46 mg (25%), viscous oil. $R_f$: 0.42 ($CHCl_3$/MeOH, 4:1). IR ($cm^{-1}$) *ν:* 3500−3100, 1630. TSP: 392 $(M+NH_4)^+$.

**7α** ($PNG_1^{\alpha}$): 52 mg (25%), viscous oil. $R_f$: 0.50 ($CHCl_3$/MeOH, 4:1). IR ($cm^{-1}$) *ν*: 3600−3100, 1600. TSP: 413 $(M+H)^+$.

**7*β*** ($PNG_1^{\beta}$): 62 mg (30%), yellow crystals. Mp: 69−70 °C. $R_f$: 0.47 ($CHCl_3$/MeOH, 4:1). IR ($cm^{-1}$) *ν*: 3600−3100, 1600. TSP: 413 $(M+H)^+$.

*Synthesis of Spin-Labeled Galactopyranoside- and Glucopyranoside-Containing Nitrophenyl Moiety. General Procedure (**9α**, **9*β***, **11α**, **19*β***) (Figure 2).* To a solution of sugar (sodium salt of **1α** or **1*β***; 109 mg, 0.5 mmol) in water (2 mL), a solution of **8** or **10** (1.0 mmol) in dioxane (4 mL) was added, and the mixture was allowed to stand overnight at room temperature. The solution was then evaporated in vacuo to dryness, and the residue was purified by flash column chromatography (hexane/EtOAc, $CHCl_3$/MeOH) to give the product **9α**, **9*β***, **11α**, or **19*β***.

**9α** ($NNG_0^{\alpha}$): 80 mg (36%), yellow crystals. Mp: 90−92 °C. $R_f$: 0.50 ($CHCl_3$/MeOH, 4:1). IR ($cm^{-1}$) *ν*: 3600−3100, 1590, 1500. TSP: 461 $(M+NH_4)^+$.

**9*β*** ($NNG_0^{\beta}$): 100 mg (45%), yellow crystals. Mp: 107−108 °C. $R_f$: 0.42 ($CHCl_3$/MeOH, 4:1). IR ($cm^{-1}$) *ν*: 3600−3100, 1590, 1500. TSP: 461 $(M+NH_4)^+$.

**11α** ($BNG_0^{\alpha}$): 72 mg (30%), yellow crystals. Mp: 116−118 °C. $R_f$: 0.46 ($CHCl_3$/MeOH, 4:1). IR ($cm^{-1}$) *ν*: 3600−3100, 1660, 1610, 1590, 1500. TSP: 501 $(M+NH_4)^+$.

**19*β*** ($NNGlu_0^{\beta}$): 71 mg (32%), yellow crystals. Mp: 135−137 °C. $R_f$: 0.54 ($CHCl_3$/MeOH, 4:1). IR ($cm^{-1}$) *ν*: 3600−3100, 1600, 1520. TSP: 461 $(M+NH_4)^+$.

*Synthesis of 1-Oxyl-2,5,5-trimethyl-2-[3-nitro-4-(N-methyl)-N−(ethyl-1-thio-β-(-D-galactopyranosid-1-yl)]aminophenyl Pyrrolidine (**13b*β***, $NNG_2^{\beta}$) (Figure 2B).* To solution of **8** (2,67 g, 10.0 mmol) in EtOH (10 mL), *N*-methyl ethanolamine (2.25 g, 30.0 mmol) was added, and the mixture was allowed to stand overnight at room temperature. The ethanol was evaporated, the residue was dissolved in $CHCl_3$ (30 mL) and washed with brine (10 mL), the organic phase was separated, dried over $MgSO_4$, and filtered, and the solvent was evaporated in vacuo. The residue was purified by flash column chromatography to give **12a** as an orange oil [Yield: 2.09 g (65%). $R_f$: 0.24 ($CHCl_3$/$Et_2O$, 2:1). IR ($cm^{-1}$) *ν*: 3400, 1610, 1510]. To the mixture of **12a** (1.93 g, 6.0 mmol) and $Et_3N$ (707 mg, 7.0 mmol) in $CH_2Cl_2$ (20 mL), methanesulfonyl chloride (801 mg, 7.0 mmol) was added dropwise at 0 °C, and the mixture was stirred for 1 h at room temperature. The organic phase was washed with brine, dried over $MgSO_4$, and filtered, and the solvent was evaporated. The residue was immediately dissolved in THF (40 mL), NaI (1.59 g, 10 mmol) was added, and the mixture was stirred and refluxed for 2h. After being cooled, $Et_2O$ (20 mL) was added, the organic phase was washed with brine (20 mL), dried over $MgSO_4$, and filtered, and the solvent was evaporated under vacuum. The residue was purified by flash column chromatography (hexane/EtOAc) to give **12b** as dark red crystals [Yield: 880 mg (34%). Mp: 57−58 °C. $R_f$: 0.52 (hexane/EtOAc, 2:1). IR ($cm^{-1}$) *ν*: 1600, 1510]. To a stirred solution of tetraacetyl-*β*-D-galactopyranosyl-isothiouronium bromide (974 mg, 2.0 mmol) in $H_2O$ (10 mL), **12b** (864 mg, 2.0 mmol) in acetone (10 mL) and $K_2CO_3$ (552 mg, 4.0 mmol) was added in one portion. The mixture was then stirred vigorously for 2 h at room temperature, the acetone was evaporated off, the residue was extracted with $CHCl_3$ (2 × 20 mL), the organic phase was dried over $MgSO_4$ and filtered, and the solvent was evaporated in vacuo. Purification by flash chromatography gave **13a*β*** as orange crystals [Yield: 694 mg (52%). Mp: 63−64 °C. $R_f$: 0.38 ($CHCl_3$/$Et_2O$, 2:1). IR ($cm^{-1}$) *ν*: 1750,1730, 1600, 1500]. A solution of **13a*β*** (668 mg, 1.0 mmol) in MeOH (10 mL) was treated with sodium methoxide (60 mg Na in 5 mL MeOH) and allowed to stand at room temperature for 2 h. The organic solvent was evaporated, a saturated aqueous solution of $NH_4Cl$ was added to the residue, and the water was evaporated in vacuo to dryness. The resulting residue was dissolved in MeOH (10 mL), filtered, and evaporated again, and the residue was purified by flash column chromatography to give **13b*β*** ($NNG_2^{\beta}$) as orange crystals [Yield: 150 mg (30%). Mp: 72−73 °C. $R_f$: 0.52 ($CHCl_3$/MeOH, 4:1). IR ($cm^{-1}$) *ν*: 3600−3100, 1600, 1510. TSP: 501 $(M+H)^+$].

*Synthesis of 1-Oxyl-2,5,5-trimethyl-2-[3-nitro-4-N−(hexyl-1-thio-β-D-galactopyranosid-1-yl)]aminophenyl Pyrrolidine (**15*β***, $NNG_6^{\beta}$) (Figure 2B).* To a stirred solution of 6-aminohexyl 1-thio-*β*-D-galactopyranoside (50 mg, 0.18 mmol) in 5% aq. $K_2CO_3$ solution (2 mL), **8** (133 mg, 0.5 mmol) was added in dioxane (4 mL), and the mixture was allowed to stand overnight at room temperature. The solvent was removed under vacuum, and the residue was purified by flash column chromatography (hexane/EtOAc, $CHCl_3$/MeOH) to give **15*β*** ($NNG_6^{\beta}$) as an orange viscous oil [Yield: 24 mg (25%). $R_f$: 0.57 ($CHCl_3$/MeOH, 4:1). IR ($cm^{-1}$), *ν*: 3600−3100, 1600, 1510. TSP: 543 $(M+H)^+$].

*Synthesis of 1-Oxyl-2,2,5,5-tetramethyl-3-formyl-4-(1-thio-D-galactopyranosid-1-yl)-2,5-dihydro-1H-pyrrole (**17α**, **17*β***).* General Procedure (Figure 2B). To a solution of sugar (sodium salt of **1α** or **1*β*** 109 mg, 0.5 mmol) in water (2

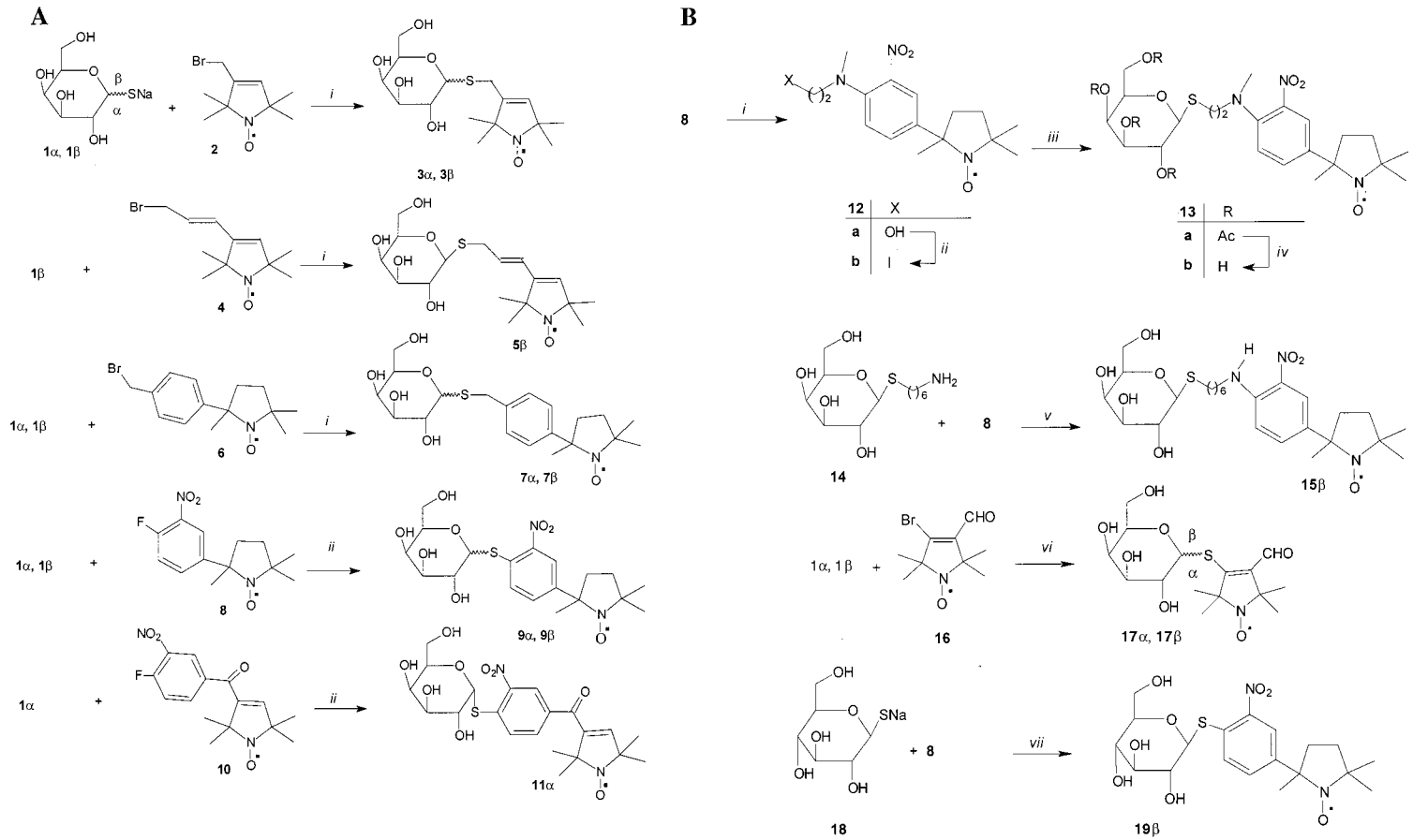


FIGURE 2: Synthetic scheme for the nitroxide spin-labeled galactopyranosides. (A) Reagents and conditions: (i) dioxane/$H_2O$, 90 °C, 1 h, 25−48%; (ii) dioxane/$H_2O$, room temperature, 12 h, 30−45%. See Experimental Procedures. (B) Reagents and conditions: (i) *N*-methyl-ethanolamine, EtOH, room temperature, 12 h, 65%; (ii) MsCl, $Et_3N$, $CH_2Cl_2$, 0 °C → room temperature, 1 h, then NaI, THF, 66 °C, 2 h, 34%; (iii) tetraacetyl-*β*-D-galacto-pyranosyl isothiouronium bromide, $K_2CO_3$, $H_2O$, acetone, room temperature, 2 h, 52%; (iv) $NaOCH_3$, $CH_3OH$, room temperature, 2 h, 30%; (v) dioxane, 5% aq. $K_2CO_3$, room temperature, 12 h, 25%; (vi) dioxane/$H_2O$, room temperature, 2 h, 27−39%; (vii) dioxane/$H_2O$, room temperature, 12 h, 32%. See Experimental Procedures.

mL), a solution of **16** (150 mg, 0.6 mmol) in dioxane (4 mL) was added, and the mixture was allowed to stand at room temperature for 2 h. The solution was then evaporated in vacuo to dryness, and the residue was purified by flash column chromatography (hexane/EtOAc, $CHCl_3$/MeOH) to give **17α** or **17*β***.

**17α** ($fNG_0^{\alpha}$): 48 mg (27%), orange crystals. Mp: 110−112 °C. $R_f$: 0.35 ($CHCl_3$/MeOH, 4:1). IR ($cm^{-1}$) $\nu$: 3550−3100, 1640, 1570. TSP: 364 $(M+2H)^+$, (as N−OH).

**17*β*** ($fNG_0^{\beta}$): 70 mg (39%), orange crystals. Mp: 124−126 °C. $R_f$: 0.27 ($CHCl_3$/MeOH, 4:1). IR ($cm^{-1}$) $\nu$: 3550−3100, 1640, 1570. TSP: 364 $(M+2H)^+$, (as N−OH).

*Plasmid Construction.* Plasmid pT7−5/cassette *lacY* encoding wild-type or single-Cys148 permease with the biotin acceptor domain from a *Klebsiella pneumoniae* carboxylase was constructed as described previously (*11*).

*Growth of Cells. E. coli* T184 (*lacZ*$^-$*Y*$^-$) transformed with a given plasmid was grown aerobically at 37 °C in 1 L of Luria−Bertani broth containing streptomycin (10 μg/mL) and ampicillin (100 μg/mL) (*27*). Overnight cultures were diluted into 12 L and grown aerobically for 2 h before induction with 0.3 mM *i*-propyl 1-thio-*β*-D-galactopyranoside. After additional growth for 2 h, cells were harvested and used for membrane preparation.

*Lactose Transport.* Transport of [1-$^{14}$C]lactose (10 mCi/mmol) at a final concentration of 0.4 mM by right-side-out (RSO) membrane vesicles (*28*, *29*) was assayed under oxygen in the presence of 20 mM potassium ascorbate and 0.2 mM phenazine methosulfate (PMS) (*30*, *31*).

*Permease Purification.* Membranes prepared as described (*24*) were solubilized with 2% *n*-dodecyl-*β*-D-maltoside (DDM), and the permease was purified by avidin affinity chromatography essentially as described (*11*). Briefly, the DDM-soluble fraction was mixed with avidin−Sepharose for 30 min at 4 °C with continuous rotation. The slurry was then packed into a small column, and unbound material was removed by washing extensively with 50 mM potassium phosphate ($KP_i$; pH 7.5)/1 mM EDTA/10% glycerol/0.016% DDM (w/v) (column buffer). The permease was then eluted with 5 mM *d*-biotin in column buffer and concentrated by using a Micro-ProDiCon membrane (Spectrum Medical Industries, Houston, TX). Purified protein was analyzed by sodium dodecyl sulfate/12% polyacrylamide gel electrophoresis (*33*) and visualized by Coomassie blue staining. Protein was assayed by using a Micro BCA kit (Pierce Inc., Rockford, IL).

*MIANS Labeling of Single-Cys148 Permease.* Labeling of purified single-Cys148 permease with MIANS was performed as described (*11*).

*EPR of Spin-Labeled Galactosides*. Freshly purified wild-type permease at 100 μM final concentration in the column buffer was preincubated with a given nitroxide spin-labeled galactoside at final concentrations ranging from 4 to 400 μM for 1 min. EPR spectra were acquired at room temperature on a Varian E−109 X-band spectrometer fitted with a loop-gap resonator with samples contained in Pyrex capillaries. Each spectrum was an average of four scans over 100 G using 2 mW incident microwave power. The peak-to-peak free spin amplitude of the upfield resonance ($m_I = -1$) was used to estimate the concentration of free nitroxide spin-labeled galactopyranoside (*34*). A standard curve plotted from a series of concentrations of free nitroxide spin-labeled galactopyranosides in column buffer was used to calculate the concentration.

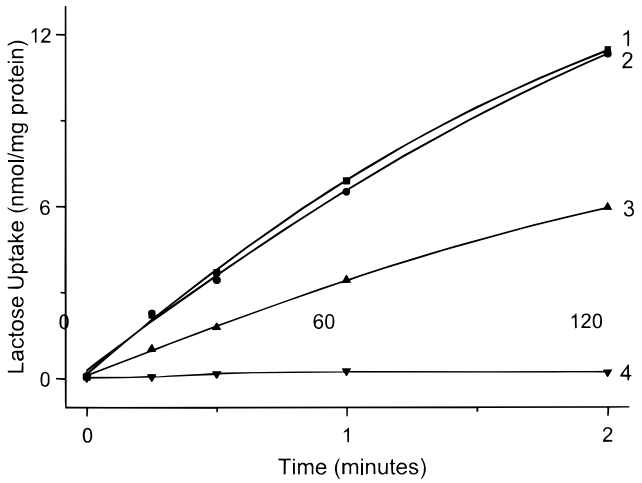


FIGURE 3: Inhibition of active lactose transport by RSO *E. coli* membrane vesicles containing wild-type permease by spin-labeled galactosides. Time courses of [1-$^{14}$C]lactose transport were assayed as described in Experimental Procedures. Key: ■, no additions or 4 mM sucrose; ●, 2 mM $NNGlu_0^{\beta}$; ▲, 10 μM $NNG_6^{\beta}$; ▼, membrane vesicles devoid of lac permease (i.e., prepared from *E. coli* T184 transformed with vector containing no *lacY* insert).

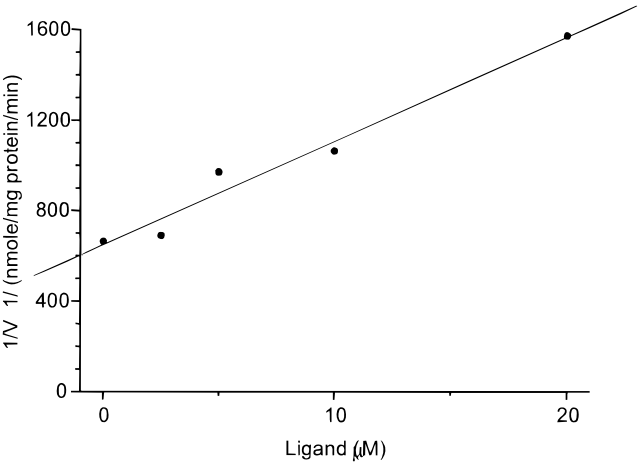


FIGURE 4: Dixon plot of the reciprocal of the initial rate of transport versus the concentrations of $NNG_6^{\beta}$. Experiments were carried out as described in Figure 3 and in Experimental Procedures.

## RESULTS

*Lactose Transport*. Representative data showing rates of lactose transport by RSO membrane vesicles in the presence of given concentrations of sucrose, $NNGlu_0^{\beta}$, or $NNG_6^{\beta}$ demonstrate clearly that $NNG_6^{\beta}$ causes about 50% inhibition at a concentration of 10 μM, while neither of the other sugars inhibits significantly at much higher concentrations (Figure 3). Therefore, as shown previously (*10*, *11*, *16*), the specificity of the permease is directed toward the galactosyl moiety of the substrate. Results from a systematic study in which initial rates of lactose transport were measured at various concentrations of $NNG_6^{\beta}$ yield a $K_I$ of about 7 μM (Figure 4). $K_I$'s for the other galactopyranosides determined in similar fashion are summarized in Table 1, and it is apparent that $NNG_6^{\beta}$ has the highest apparent affinity (i.e., lowest $K_I$) of the compounds synthesized.

Table 1: Binding of the Spin-Labeled Sugars to Lac Permease[a]

| ligand | $K_I$ ($\mu$M) | $K_{1/2}$ ($\mu$M) | $K_D$ ($\mu$M) | *n* |
|---|---|---|---|---|
| $NNG_6^\beta$ | 7 | 12 | 22 | 0.97 |
| $NNG_2^\beta$ | 22 | 32 | 56 | 0.97 |
| $PNG_1^\beta$ | 57 | 56 | 62 | 0.98 |
| $PNG_1^\alpha$ | 72 | 80 | 77 | 0.98 |
| $NNG_0^\alpha$ | 129 | 100 | 139 | 0.98 |
| $NNG_0^\beta$ | 408 | 356 | >500 | n.d. |
| $NNGlu_0^\beta$ | >4000 | >2000 | >500 | n.d. |
| $BNG_0^\alpha$ | >4000 | >2000 | >500 | n.d. |
| $NG_3^\beta$ | >4000 | >2000 | >500 | n.d. |
| $NG_1^\beta$ | 580 | >2000 | >500 | n.d. |
| $NG_1^\alpha$ | >4000 | >2000 | >500 | n.d. |
| $fNG_0^\beta$ | >4000 | >2000 | >500 | n.d. |
| $fNG_0^\alpha$ | >4000 | >2000 | >500 | n.d. |

[a] $K_I$ is determined from the inhibition profile of [$^{14}$C]lactose transport by RSO membrane vesicles. Initial rates were plotted versus concentrations of given spin-labeled ligands to derive $K_I$ values (Figure 3). $K_{0.5}$ is estimated from the initial rate of fluorescence change upon mixing MIANS (10 $\mu$M, final concentration) with purified single-Cys148 permease (100 $\mu$g protein/mL, final concentration). Initial rates were plotted versus concentration of a given nitroxide spin-labeled ligand, and the concentration yielding a 50% decrease in initial rate was taken as the value of $K_{0.5}$ (Figure 6). $K_D$, the equilibrium dissociation constant, and *n*, the stoichiometry, is determined from the difference in the free spin amplitude in the absence and presence of TDG at varying the concentrations of a given nitroxide spin-labeled ligand (see *26*). Values for $K_D$ and *n* were derived from Scatchard plots (Figure 8). n.d.*:* not determined.

*MIANS Labeling of Single-Cys148 Permease*. Cys148 (helix V) which is in the binding site of the permease interacts hydrophobically with the galactosyl moiety of substrate (*10*, *11*, *16*) and is protected from alkylation by MIANS and other alkylating agents. MIANS is not fluorescent until the maleimido group reacts with a thiol side-chain (*35*, *36*), making it a convenient reagent for studying ligand protection against alkylation of Cys148 (*11*, *29*, *38*). In a representative experiment, the effect of given sugars on the time course of MIANS fluorescence with single-Cys148 permease is shown (Figure 5). Neither sucrose nor $NNGlu_0^\beta$ at high concentrations has a significant effect, but the increase in fluorescence observed in the presence of $NNG_0^\alpha$ or $NNG_6^\beta$ is inhibited by 20% or 80% at concentrations of 50 or 10 $\mu$M, respectively. The apparent affinity of single-Cys148 permease for given sugars was estimated from the concentration that yields 50% inhibition of the initial rate of increase in MAINS fluorescence (*37*) ($K_{0.5}$; Figure 6). For $NNG_0^\alpha$ and $NNG_6^\beta$, $K_{0.5}$ values of 129 and 12 $\mu$M, respectively, are obtained. $K_{0.5}$ values obtained for the other spin-labeled sugars in a similar fashion are summarized in Table 1.

*Spin-Labeled Galactoside Binding by EPR*. The spin of the unpaired electron of a nitroxide free radical typically displays three resonance lines due to coupling with the nitrogen nucleus ($I = 1$), and this is the case with the spin-labeled galactosides described here (not shown). In aqueous solution, the motion of the spin-labeled galactopyranosides is sufficiently rapid to average magnetic anisotropy, and the isotropic motion gives rise to narrow, intense resonance lines. However, binding to a large molecule such as lac permease results in a decrease in motional freedom and broadening of the resonance lines (*34*). Since the upfield resonance ($m_I = -1$) contains almost all the free spin amplitude, this line is used to illustrate the effect of binding on the EPR spectrum of the spin-labeled galactosides (Figure 7). As shown, the amplitude of the free spin label decreases by about 60% in the presence of purified wild-type permease in DDM (Figure 7). Importantly, approximately 40% of the signal is recovered upon addition of a saturating concentration of $\beta$-D-galactopyranosyl 1-thio-$\beta$-D-galactopyranoside (TDG), a high-affinity ligand with no spin label, but no effect is observed upon addition of sucrose. Thus, although there is a significant nonspecific binding component (ca. 30% of the total signal), approximately 70% of the decrease in amplitude represents

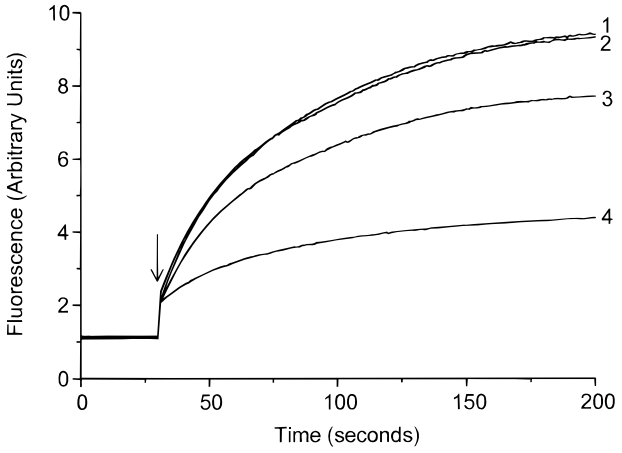


FIGURE 5: Blockade of labeling of purified single-Cys148 permease by MIANS. Time courses of MIANS fluorescence increase were recorded in 0.4 mL of 50 mM $KP_I$ (pH 7.5)/1 mM EDTA/10% glycerol/0.016% DDM (w/v) and 100 $\mu$g/mL freshly purified single-Cys148 permease. The reaction was initiated by adding MIANS to a final concentration of 10 $\mu$M, and fluorescence was recorded continuously at 415 nm (excitation at 330 nm). Key: curve 1, no addition or 4 mM sucrose; curve 2, 2 mM $NNGlu_0^\beta$; curve 3, 50 $\mu$M $NNG_0^\alpha$; curve 4, 10 $\mu$M $NNG_6^\beta$.

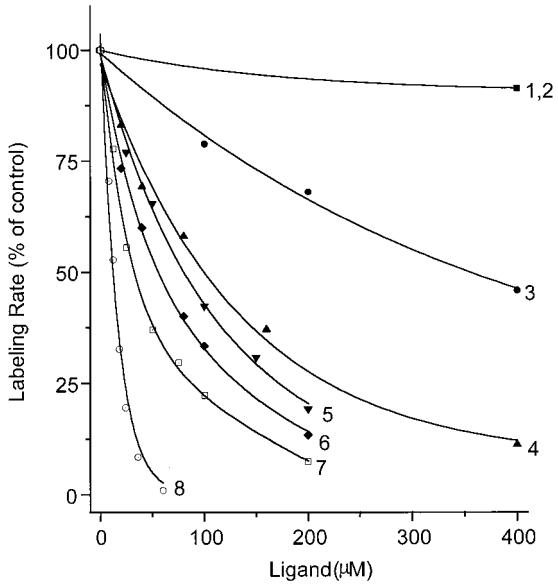


FIGURE 6: Half-maximal blockade of MIANS fluorescence changes by given spin-labeled galactopyranosides. $K_{0.5}$'s of the spin-labeled galactopyranosides were determined from the ligand concentration that yields 50% blockade of the MIANS labeling rate relative to a control sample. Key: curve 1, sucrose; curve 2, $NNGlu_0^\beta$; curve 3, $NNG_0^\beta$; curve 4, $NNG_0^\alpha$; curve 5, $PNG_1^\alpha$; curve 6, $PNG_1^\beta$; curve 7, $NNG_2^\beta$; curve 8, $NNG_6^\beta$.

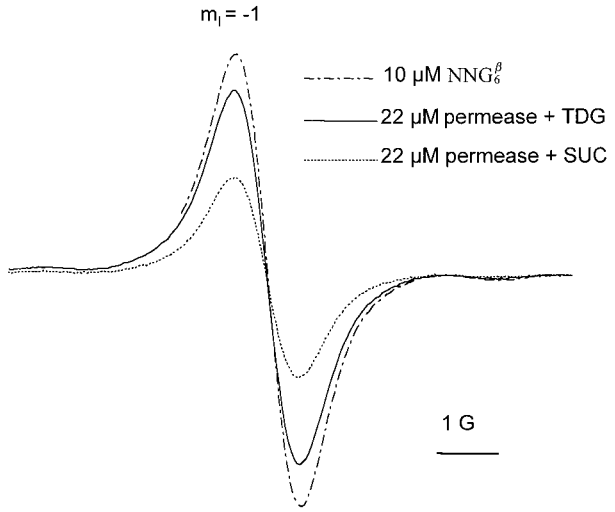


FIGURE 7: Binding of $NNG_6^\beta$ measured by EPR. EPR spectra were recorded in 10 $\mu$L of solution containing 50 mM $KP_i$ (pH 7.5)/1 mM EDTA/10% glycerol/2% DDM (w/v) with 22 $\mu$M freshly purified wild-type permease as described in Experimental Procedures. As indicated, spectra were obtained with 10 $\mu$M $NNG_6^\beta$ alone or in the presence of 22 $\mu$M purified lac permease with either 20 mM sucrose which does not bind to the permease or TDG, a high-affinity ligand. The upfield resonance ($m_I = -1$) represents essentially free spin-labeled $NNG_6^\beta$. The difference in amplitude between the signals obtained in the presence of permease and sucrose or TDG is used to quantify the amount of ligand bound to the permease.

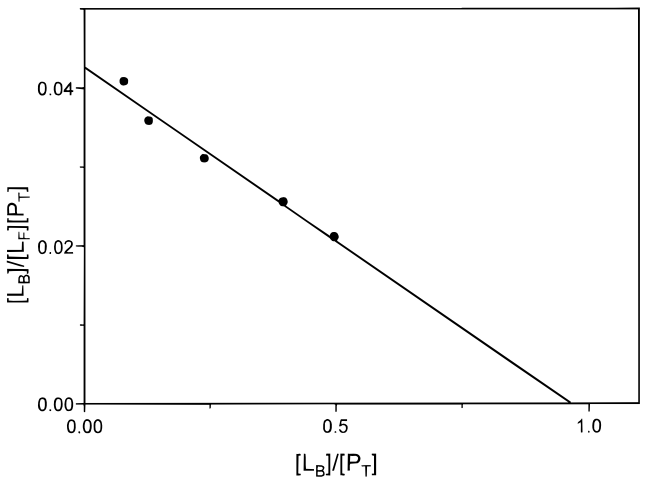


FIGURE 8: $NNG_6^\beta$ binding to lac permease. Experiments were carried out with 22 $\mu$M purified lac permease and various concentrations of $NNG_6^\beta$ as described in Figure 7 and Experimental Procedures and plotted according to Scatchard (*31*). $[L]_F$ is the free $NNG_6^\beta$ concentration; $[L]_B$ is the bound $NNG_6^\beta$ concentration calculated from the difference in amplitude between spectra obtained in the presence of 20 mM sucrose or 20 mM TDG (see Figure 7); $[P]_T$ is the total protein concentration.

specific binding to the permease. In an effort to investigate further the nonspecific component, EPR spectra of $NNG_6^\beta$ were obtained in buffer in the absence or presence of 2% DDM, the final concentration estimated to be present in the purified permease preparation. Although not shown, the amplitude of $NNG_6^\beta$ is reduced by about 10% in the presence of DDM. Therefore, approximately half of the nonspecific component represents binding to DDM micelles, and the other half represents nonspecific binding to DDM micelles containing the permease.

The equilibrium dissociation constant ($K_D$) and number of binding sites for $NNG_6^\beta$ were obtained by quantifying the differences in the amplitude of spectra obtained at various concentrations of $NNG_6^\beta$ in the absence and presence of a saturating concentration of TDG and plotting the difference according to Scatchard (*39*) (Figure 8). A $K_D$ of about 22 $\mu$M is observed with a binding stoichiometry ($n$) approximating unity. $K_D$'s and binding stoichiometries for the other spin-labeled sugars are given in Table 1.

## DISCUSSION

In an attempt to localize further the substrate binding site in lac permease, 12 nitroxide spin-labeled α- or $\beta$-galactopyranosides have been synthesized and characterized with respect to affinity for the permease. In addition, a spin-labeled $\beta$-glucopyranoside was synthesized as a control for specificity. The findings indicate that although a number of the spin-labeled galactopyranosides bind to the permease in a specific fashion, $NNG_6^\beta$ appears to do so with the highest affinity and therefore is most appropriate for further studies.

As shown with *N*-(dansyl-aminoalkyl)-$\beta$,D-galactopyranosides (reviewed in *18*), the affinity of the permease for ligand increases with longer and more hydrophobic alkyl linkers between the galactoside and dansyl moieties. A similar situation is apparent with the spin-labeled galactosides (Table 1). Thus, $NNG_6^\beta$ with a hexyl side-chain and a nitrophenyl group inhibits lactose transport with a lower $K_i$, exhibits a lower $K_{0.5}$ with respect to blockade of MIANS labeling, and has a $K_D$ as determined by EPR lower than the $NNG_0^\beta$ which contains only the nitrophenyl group. In turn, by all three criteria, $NNG_0^\beta$ exhibits an affinity higher than that of $NG_1^\beta$ with a single methyl group as a linker. Another important property with respect to affinity is the galactosidic linkage (i.e., α versus $\beta$). Generally, α-galactopyranosides exhibit higher affinity for the permease than do the $\beta$ analogues (see *16*). Consistently, $NNG_0^\alpha$ exhibits more than 3-fold better affinity than that of $NNG_0^\beta$, although neither inhibits as effectively as $NNG_6^\beta$. However, $PNG_1^\alpha$ and $PNG_1^\beta$ exhibit comparable affinities, indicating that to some extent, the nature of the anomeric substituent influences the effect of the configuration of the galactosidic linkage.

The correlation between the structures of the ligand and their relative affinities supports the contention (*11*, *16*) that the galactosyl moiety of the substrate is the primary determinant for specificity, whereas the anomeric substituent can increase affinity by nonspecific hydrophobic interactions with the protein. Thus, galactose is the most specific ligand but binds with an affinity of only 30 mM, whereas $NNG_6^\beta$ which contains a hexyl chain, as well as a nitrophenyl group, as a linker has an affinity in the low micromolar range.

The finding that binding of a number of the spin-labeled galactosides to the permease can be detected by EPR (Figure 7; Table 1) is particularly noteworthy, as the intent of these studies is to identify spin-labeled ligands that bind to the permease in such a manner that spin−spin interactions between the bound ligand and spin-labeled single-Cys replacements in the permease can be used to localize the binding site more precisely. The effect of ligand binding to the permease on the mobility of the spin-labeled galactosides is observed directly by EPR. In aqueous solution at room

temperature, the motion of the free spin-labeled galactopyranosides is sufficiently rapid to average the anisotropy, and three equally narrow and intense lines are observed. However, binding to permease decreases motion so that there is incomplete averaging of anisotropy, and the resonance lines appear broad and decreased in amplitude. Since the upfield resonance line ($m_I = -1$) represents the spin amplitude of essentially the freely mobile nitroxide only, this line is used to estimate the effect of binding on the resonance of the free spin-labeled galactopyranosides (Figure 7). Clearly, with $NNG_6^\beta$, the amplitude of the free spin labeled galactoside is markedly decreased in the presence of wild-type permease. Most importantly, this effect is reversed to a large extent by addition of TDG, demonstrating that $NNG_6^\beta$ binds to the permease in a specific fashion. Furthermore, sucrose which is not a substrate for the permease has no effect. However, about a third of the total decrease in amplitude is due to nonspecific binding. Although the amount of nonspecific binding is significant, it represents a relatively small percentage of the total signal, and specific binding can readily be quantified from the increase in amplitude observed in the presence of TDG. Thus, it is clear from the data presented in Table 1 that the $K_D$'s obtained for the ligands that bind with relatively high affinity ($NNG_6^\beta$, $NNG_2^\beta$, $PNG_1^\beta$, $PNG_1^\alpha$, and $NNG_0^\alpha$) correlate reasonably well with the $K_I$'s and apparent $K_{0.5}$'s obtained for inhibition of lactose transport and blockade of MIANS labeling of Cys148, respectively.

The spin-labeled galactosides that bind with relatively high affinity can now be used to localize the binding site in the permease more specifically. Studies on spin−spin interactions between different spin-labeled galactosides and spin-labeled Cys residues at the interface between helices IV and V, as well as other regions of the permease, are currently in progress.

## REFERENCES


1. Kaback, H. R. (1986) *Ann. Rev. Biophys. Biophys. Chem. 15*, 279−319.
2. Müller-Hill, B. (1996) *The lac Operon: A Short History of a Genetic Paradigm*, Walter de Gruyter, Berlin, New York.
3. Viitanen, P., Newman, M. J., Foster, D. L., Wilson, T. H., and Kaback, H. R. (1986) *Methods Enzymol. 125*, 429−452.
4. Sahin-Tóth, M., Lawrence, M. C., and Kaback, H. R. (1994) *Proc. Natl. Acad. Sci. U.S.A. 91*, 5421−5425.
5. Kaback, H. R. (1996) in *Handbook of Biological Physics: Transport Processes in Eukaryotic and Prokaryotic Organisms* (Konings, W. N., Kaback, H. R., and Lolkema, J. S., Eds.) pp 203−227, Elsevier, Amsterdam.
6. Kaback, H. R., Voss, J., and Wu, J. (1997) *Curr. Opin. Struct. Biol. 7*, 537−542.
7. Kaback, H. R., and Wu, J. (1997) *Quart. Rev. Biophys. 30*, 333−364.
8. Frillingos, S., Sahin-Tóth, M., Wu, J., and Kaback, H. R. (1998) *FASEB J. 12*, 1281−1299.
9. Kaback, H. R., and Wu, J. (1999) *Acc. Chem. Res. 32*, 805−813.
10. Jung, H., Jung, K., and Kaback, H. R. (1994) *Biochemistry 33*, 12160−12165.
11. Wu, J., and Kaback, H. R. (1994) *Biochemistry 33*, 12166−12171.
12. Frillingos, S., Gonzalez, A., and Kaback, H. R. (1997) *Biochemistry 36*, 14284−14290.
13. Venkatesan, P., and Kaback, H. R. (1998) *Proc. Natl. Acad. Sci. U.S.A. 95*, 9802−9807.
14. Sahin-Tóth, M., le Coutre, J., Kharabi, D., le Maire, G., Lee, J. C., and Kaback, H. R. (1999) *Biochemistry 38*, 813−819.
15. Zhao, M., Zen, K.-C., Hubbell, W., and Kaback, H. R. (1999) *Biochemistry 38*, 7407−7412.
16. Sahin-Tóth, M., Akhoon, K. M., Runner, J., and Kaback, H. R. (2000) *Biochemistry 39*, 5097−5103.
17. Weinglass, A. B., and Kaback, H. R. (1999) *Proc. Natl. Acad. Sci. U.S.A. 96*, 11178−11182.
18. Schuldiner, S., and Kaback, H. R. (1977) *Biochim. Biophys. Acta 472*, 399−418.
19. Gnewuch, T., and Sosnovsky, G. (1986) *Chem. Rev. 86*, 203−238.
20. Schmidt, R. R., and Stumpp, M. (1983) *Liebigs Ann. Chem.* 1249−1256.
21. Hankovszky, H. O., Hideg, K., and Lex, L. (1980) *Synthesis* 914−916.
22. Hankovszky, H. O., Hideg, K., Lovas, M. J., Jerkovich, Gy., Rockenbauer, M., Gyôr, M., and Sohár, P. (1989) *Can. J. Chem. 67*, 1392−1400.
23. Kálai, T., Balog, M., Jekõ, J., and Hideg, K. (1998) *Synthesis* 1479−1482.
24. Bonner, W. A., and Kahn, J. E. (1951) *J. Am. Chem. Soc. 73*, 2241−2245.
25. Slama, J., and Rando, R. R. (1981) *Carbohydr. Res. 88*, 213−221.
26. Zemplén, G. (1926) *Chem. Ber. 59*, 2402−2413.
27. Teather, R. M., Bramhall, J., Riede, I., Wright, J. K., Furst, M., Aichele, G., Wilhelm, V., and Overath, P. (1980) *Eur. J. Biochem. 108*, 223−231.
28. Kaback, H. R. (1971) *Methods Enzymol. 22*, 99−120.
29. Short, S. A., Kaback, H. R., and Kohn, L. D. (1975) *J. Biol. Chem. 250*, 4291−4296.
30. Konings, W. N., Barnes, E. M., Jr., and Kaback, H. R. (1971) *J. Biol. Chem. 246*, 5857−5861.
31. Kaback, H. R. (1974) *Methods Enzymol. 31*, 698−709.
32. Viitanen, P., Garcia, M. L., and Kaback, H. R. (1984) *Proc. Natl. Acad. Sci. U.S.A. 81*, 1629−1633.
33. Newman, M. J., Foster, D. L., Wilson, T. H., and Kaback, H. R. (1981) *J. Biol. Chem. 256*, 11804−11808.
34. Cafiso, D. S., and Hubbell, W. L. (1981) *Ann. Rev. Biophys. Bioeng. 217*, 217−244.
35. Gupte, S. S., and Lane, L. K. (1979) *J. Biol. Chem. 254*, 10362−10369.
36. Haugland, R. P. (1994) *Handbook of Fluorescent Probes and Research Chemicals*, 5th ed., Molecular Probes Inc., Eugene, OR.
37. He, M., and Kaback, H. R. (1997) *Biochemistry 36*, 13688−13692.
38. le Coutre, J., Whitelegge, J. P., Gross, A., Turk, E., Wright, E. M., Kaback, H. R., and Faull, K. F. (2000) *Biochemistry 39*, 4237−4242.
39. Scatchard, G. (1949) *Ann. N.Y. Acad. Sci. 51*, 660−672.


BI001075I